ARMAX-BASED MIMO PREDICTIVE CONTROL FOR MULTI-ZONE COOLING OF COMPOSITE MOLDING TOOLS

DJAMEL EDDINE GUERFI

Nantes Université, IRT Jules Verne, F-44000 Nantes, France
E-mail: djamel-eddine.guerfi@irt-jules-verne.fr

Abstract - This study presents the design and experimental validation of a model predictive control (MPC) framework for enhancing thermal uniformity in thermoplastic composite molding tools used in aeronautical, naval, and automotive applications. Building upon a previously developed hybrid cooling concept combining impinging water jets and transverse air flow, the proposed approach extends predictive control to a multi-input multi-output (MIMO) configuration integrating three Smart Elements of Cooling (SECs). Each SEC is modeled using an ARMAX-based predictor to capture coupled thermal dynamics and cross-zone interactions. The MPC employs a quadratic optimization solved by the KWIK algorithm to regulate water flow rates while maintaining constant air flow. Experimental results demonstrate significant improvements in thermal regulation performance, achieving tracking errors below 5 °C, a reduction in RMSE of up to 79.4%, and water consumption savings of 64.8% compared to conventional On–Off control. The proposed strategy confirms the effectiveness of predictive coordination for multi-zone cooling of composite forming tools.

Keywords - ARMAX, composite processing, impinging jet, model predictive control, multi-zone cooling, thermal uniformity.

I. INTRODUCTION

The thermoforming and preforming stages are crucial for thermoplastic composites, as fibre positioning and thermal history govern mechanical strength and structural integrity [1], [2]. Uniform temperature fields prevent resin-rich zones, voids, and defects such as warpage and residual stresses [3].

Traditional cooling technologies—usually straight drilled channels—suffer from strong thermal heterogeneity along the coolant flow due to fluid heating and phase change, causing non-uniform cooling rates [4], [5]. Conformal cooling channels improve heat transfer by enabling complex flow paths [6], [7], yet high initial mould temperatures (>200°C) still induce two-phase flow and boiling instabilities [4].

Jet impingement cooling provides superior local heat-transfer coefficients and better surface temperature control [8], [9], [10]. Guerfi et al. [11], [12], [13] introduced Smart Elements of Cooling (SECs) combining impinging water jets with transverse airflow, enhancing thermal exchange uniformity and enabling dynamic regulation.
However, when multiple SECs operate simultaneously, cross-interactions arise via thermal conduction and convective coupling between zones, complicating the regulation of local surface temperatures. To address this challenge, the present work proposes a model predictive control (MPC) strategy based on ARMAX models, capable of predicting and optimising the coupled thermal behaviour of multiple SECs. This approach extends earlier single-SEC (SISO) implementations previously developed at the laboratory [14] to a MIMO configuration, in which three SECs are regulated in coordination. Water flow rates are actively regulated, while in this study air flow is fixed — a simplification justified by experimental evidence and recent studies showing that the air-stream influence becomes secondary compared to impinging jets under high-heat flux conditions [15].

II. PRINCIPLE OF THE IMPINGING JET COOLING CONCEPT

In conventional horizontal channels, cooling efficiency decreases with distance due to boundary layer development and rising fluid temperatures. The proposed solution (See Fig. 1.) involves inserting a smaller perforated tube inside each cooling channel, closed at the outlet and drilled with multiple holes oriented upward, generating impinging jets that directly impact the inner wall.

The jet configuration optimization performed in prior work [11] established:

- Jet spacing: $dist_{jet} = (10_30)\, D_{jet}$
- Jet diameter: $D_{jet} \leq \frac{D_h}{7.5}$, where D_h is the hydraulic diameter (See Fig. 1.)

A transverse air flow between the tube and the channel outlet evacuates the air–water–vapor mixture, enhancing local heat transfer intensity by approximately 40% in jet interaction zones [16], [17].

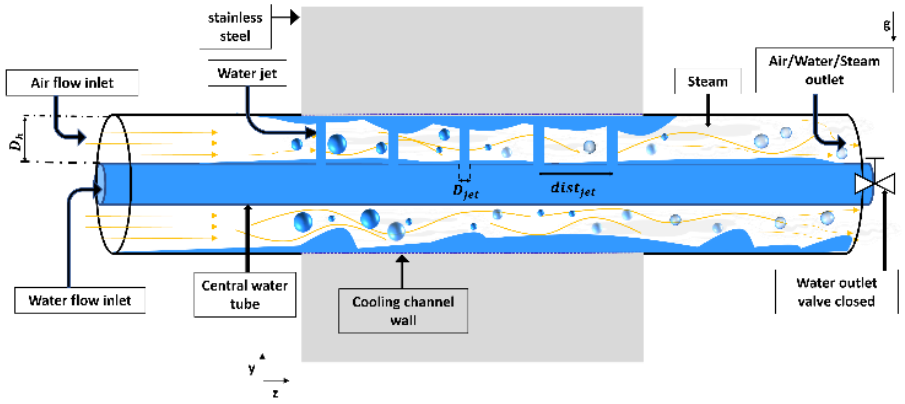

Fig. 1. Schematic representation of the impinging jet cooling principle

In this study, each cooling channel has a diameter of 27 mm, with an inner tube of 10 mm inner and 12 mm outer diameter. Seventeen 1 mm-diameter jets are distributed along the tube with 30 mm spacing, leaving a 10 mm margin at both ends.

III. EXPERIMENTAL TOOL DESIGN

The developed mold, shown in Fig. 2, consists of three parallel cooling channels embedded in an aluminum corner-shaped tooling block. Each channel contains a perforated tube following the optimized jet configuration described above. The goal is to enable independent regulation of each channel's flow to homogenize temperature across the mold surface interfacing the upper and lower halves during composite forming.

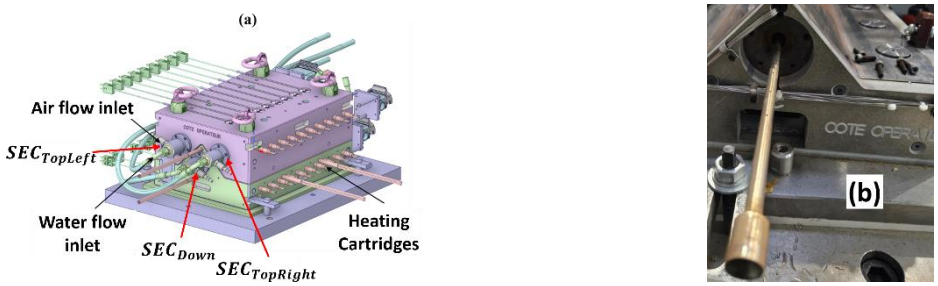

Fig. 2. 3D CAD assembly of the tooling (a) and inserted perforated cooling tube in the SEC_{down} channel wall (b).

To assess longitudinal cooling uniformity, ten thermocouples were installed 10 mm above the SEC_{down} channel wall (D) and ten other thermocouples 10 mm below the same cooling channel (C) as shown in Fig. 3.

The temperature evolution at these positions was monitored for two configurations: (i) conventional direct water cooling, and (ii) impinging jet cooling.

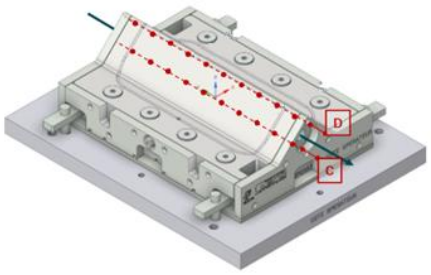

Fig. 3. Instrumentation layout of the lower part of the tooling

The standard deviation among the twenty sensors served as an indicator of longitudinal temperature homogeneity improvement (see Fig.3.) In addition, the temperature of each surface area controlled by the individual SECs was measured using four thermocouples per surface(see Fig.4.) The average temperature of these sensors was used as both the output and the control objective in the two regulation models. In practice, the flow rate is regulated among the three SECs to minimize the temperature difference between the three surface zones in contact with the molded part and the target cooling rate (TCR).

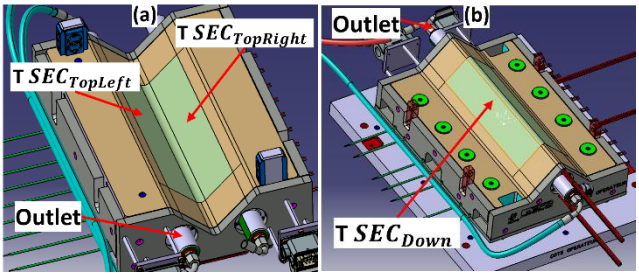

Fig.4. (a) Surfaces controlled by the left and right SEC;(b) Surface controlled by the SEC_{down}

IV. CONTROL MODEL DEVELOPMENT

A. Model Predictive Control (MPC) Operation and Computational Sequence

Model Predictive Control (MPC) determines the optimal sequence of manipulated variables (MVs) by solving a constrained optimization at each sampling instant [18]. It predicts the future process evolution over a finite horizon using current measurements of MVs, disturbance variables (DVs), and controlled variables (CVs), minimizing a quadratic cost function while respecting process and actuator constraints.

The standard MPC formulation includes four main objectives:

1. Reference tracking: minimize deviations between predicted and target CVs.
2. Actuator regularization: keep MVs near nominal values.
3. Move suppression: limit abrupt actuator changes to prevent instability.
4. Constraint handling: use slack variables to respect physical and operational limits.

The computational sequence of a typical MPC cycle is summarized in Fig. 5 [18].

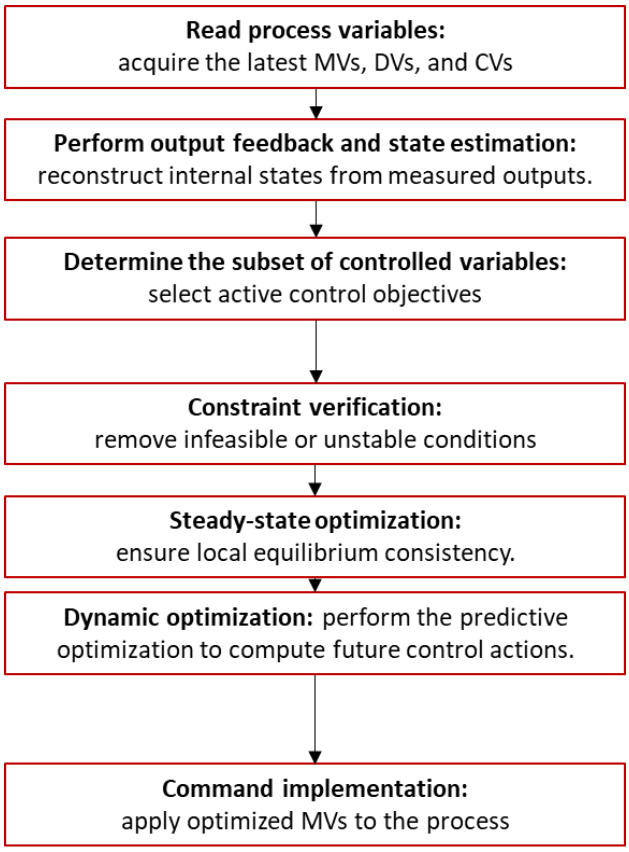

Fig. 5. Computational sequence of the MPC controller [18].

At each step, only the first element of the optimal sequence is applied (receding-horizon control), and optimization is repeated with updated measurements. This iterative approach enables MPC to anticipate system dynamics and adapt in real time to disturbances and nonlinear behaviors.

B. ARMAX Model Definition and Principles

The AutoRegressive Moving Average with eXogenous inputs (ARMAX) model is a discrete-time parametric framework widely used for system identification and predictive control [19].

It captures the relationship between system inputs, outputs, and stochastic disturbances using autoregressive, moving-average, and exogenous components.

According to Ljung [19], the ARMAX model is expressed as:

$$A(q)y(t) = B(q)u(t - n_k) + C(q)e(t) \quad (1)$$

Where $y(t)$ is the process output, $u(t)$ the input, and $e(t)$ a white-noise disturbance.

The operators $A(q)$, $B(q)$, and $C(q)$ are polynomials in the backward shift operator q^{-1}, and n_a, n_b, n_c and n_k denote the model orders and delay.

The ARMAX structure combines:

- Autoregressive (AR) terms to model system dynamics and memory,

- Moving-Average (MA) terms to represent stochastic noise, and
- Exogenous (X) inputs to incorporate external control actions.

This hybrid structure allows for highly accurate predictions of transient responses, making ARMAX ideal for integration within predictive controllers such as MPC.

C. Complementarity Between ARMAX and MPC

Combining ARMAX prediction with MPC optimization enhances control robustness and adaptability. ARMAX provides accurate multi-step-ahead temperature forecasts, which MPC uses to compute optimal flow adjustments. The autoregressive terms capture process dynamics, the moving-average component accounts for stochastic disturbances, and the exogenous inputs model cross-coupling among cooling zones, enabling coordinated temperature control. This synergy yields an adaptive, data-driven MPC architecture capable of real-time optimization under dynamic thermal conditions. The standard deviation among the twenty sensors was used as an indicator of longitudinal temperature homogeneity improvement

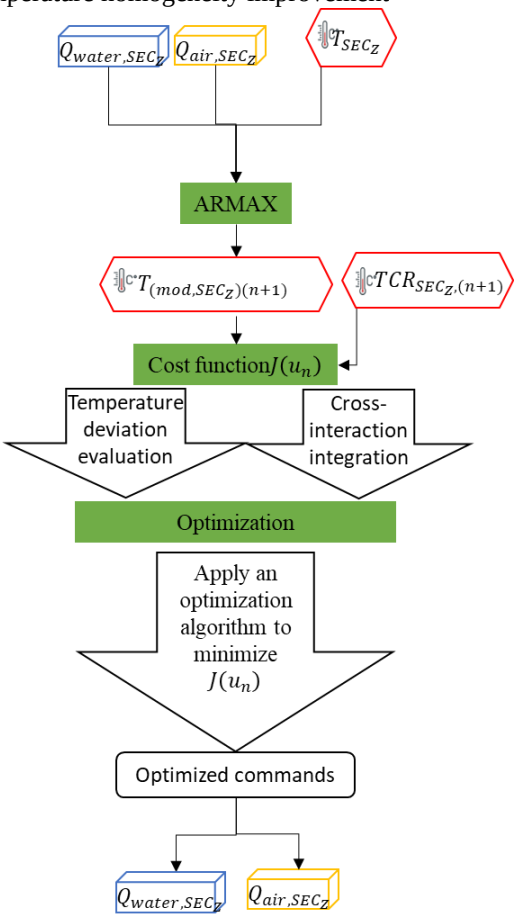

Fig. 6. Schematic representation of the MPC computational loop for three SECs, integrating ARMAX-based predictions, cost evaluation, and optimization of water and air flow commands

D. Optimization Problem and Cost Function Formulation

The MPC optimization problem aims to minimize the deviation between the predicted surface temperatures and their reference trajectories (TCR,z), while accounting for cross-coupling effects among the three cooling zones.

The cost function is defined as:

$$J(u_n) = \sum_{z=1}^{3}\sum_{i=1}^{PH}\left(\frac{W_{i,z}}{S_z}\left(TCR_z(n+i) - T_{mod,z}(n+i)\right)\right)^2 + \sum_{i=1}^{HP}\sum_{\substack{z=1 \\ j=1,j\neq z}}^{3} \alpha_{z,j}\left(T_{mod,z}(n+i) - \beta_{z,j}T_{mod,j}(n+i)\right)^2 \quad (2)$$

where:

- $J(u_n)$: total cost function to minimize at control instant (n).
- $T_{mod,z}(n+i)$: predicted surface temperature for zone (z) (SEC_z) at prediction step (i).
- $TCR_z(n+i)$: Target Cooling Rate for zone (z) at prediction step (i).
- $w_{i,z}$: weighting coefficient emphasizing the relative importance of each zone or specific prediction step.
- s_z : normalization factor ensuring balanced contributions of each zone to the total cost function.
- $\alpha_{z,j}$: global coefficient scaling the cross-coupling effect from zone (j) to zone (z).
- $\beta_{z,j}$: asymmetry factor modeling the directional thermal influence of zone (j) on zone (z). Each pair of SECs has a unique $\beta_{z,j}$ to capture non-symmetric interactions.
- (PH): prediction horizon length, i.e., number of future time steps considered in the MPC optimization.

The first term of (2) minimizes temperature-tracking errors for each SEC, while the second term penalizes discrepancies arising from inter-zone interactions, ensuring cooperative cooling performance across the surface.

The control input vector is:

$$u_n = \begin{bmatrix} u_{Down,n} \\ u_{TopRight,n} \\ u_{TopLeft,n} \\ u_{Air,Down,n} \\ u_{Air,TopRight,n} \\ u_{Air,TopLeft,n} \end{bmatrix} \quad (3)$$

- $u_{SEC,n}$: water flow rate for each SEC at control instant (n).
- $u_{AIR,SEC,n}$: air flow rate for each SEC (kept constant at 50 L/min in this study but included in

the vector for completeness).

E. MPC Control Procedure Using ARMAX Predictions

The ARMAX–MPC control process operates iteratively according to the following sequence:

1. Acquisition of process data: read real-time measurements of MVs, DVs, and CVs.
2. Prediction: compute surface temperature estimates T_{SEC} using the ARMAX model.
3. State validation: determine active control zones and ensure valid operating conditions.
4. Steady-state optimization: establish feasible reference points.
5. Dynamic optimization: minimize $J(u_n)$ to determine the optimal flow sequence.
6. Command execution: apply the optimized water flow rates to the three SECs via proportional valves.

This iterative MPC–ARMAX scheme ensures coordinated, real-time thermal management across all three SECs, achieving precise cooling control with minimal resource use.

F. Determination of Response Time

Characterizing the response time of three Smart Cooling Elements (SECs) with cross-channel interactions is essential to tune MPC parameters for optimal cooling. Pulsed water flows were applied across temperatures from 350 °C to 110 °C to determine the time constants (τ) and response times (TR) for each cooling zone.

The time constant (τ) is defined as the duration for the response to reach 63% of its final value:

$$y(t) = 1 - e^{-t/\tau} \quad (4)$$

The full response time, corresponding to 90% of the final value, is calculated as:

$$TR = 2{,}3 \times \tau \quad (5)$$

Fig. 7 illustrates the experimental setup for response time determination for each zone.

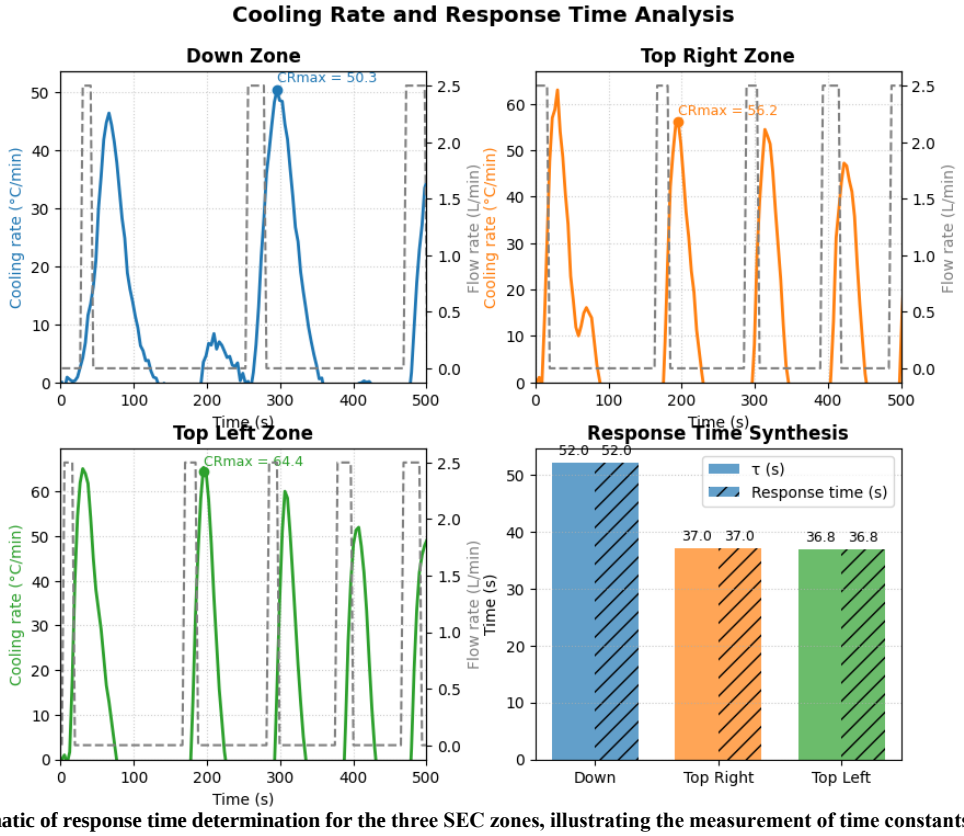

Fig. 7. Schematic of response time determination for the three SEC zones, illustrating the measurement of time constants (τ) and total response times (TR) for MPC tuning.

Synthesized response parameters for each zone are summarized in Table I.

Observations highlight dynamic response variability with repeated pulses and temperature changes. For example, after the second water pulse in the Down zone, the time to reach 63% of the maximum cooling rate slightly increased from 22.7 s to 26 s, while in the Top Right zone it increased to 28 s. The total response time for the first zone was 52 s and 59 s for the second during this second pulse. Similar variations of 10–20% were observed across all zones with temperature variations of 40–70 °C, attributed to the temperature-dependent thermal conductivity of the steel block.

Zone	Perturbation start (s)	CRmax (°C/min)	Time at CRmax (s)	63% of CRmax (°C/min)	Time to 63% (s)	TR (s)
Down	256	50	295	31	279	52
Top Right	166	56	195	35	182	37
Top Left	170	64	195	40	182	36

TableI. Synthesized response parameters for each zone

This variability demonstrates the importance of considering zone-specific dynamics and temperature ranges in MPC tuning. Accurate response time determination is critical to optimize the MPC parameters, ensuring precise control of cooling across the entire mold surface.

V. EXPERIMENTAL PROCEDURE

To train and validate the ARMAX model, the following tests were conducted:

- Graded water flow rates
- Three different opening / closing durations of water solenoid valves
- Three channel-by-channel activation sequences to assess cross-channel interactions

On–Off tests were performed with variable target cooling rates (TCR), and cross-channel coupling coefficients were extracted to calibrate the predictive model for multi-channel coordination. The controller aimed to follow a temperature rate setpoint in °C/min while minimizing water consumption.

No	Water flow (l/min)	Open-Close Duration	SECs cooled
0	0	Continuous	0
1	1	Continuous	3
2	2	Continuous	3
3	3 (Nominal Test)	Continuous	3
4	4	Continuous	3
5	5	Continuous	3
6	3	4s–40s	3
7	3	8s–40s	3
8	3	16s–40s	3
9	3	32s–40s	3
10	3	Continuous	Down
11	3	Continuous	Top Right
12	3	Continuous	Top Left
13	3	On–Off TCR 5°C/min	3
14	3	On–Off TCR 10°C/min	3
15	3	On–Off TCR 15°C/min	3

Table II. Experimental test matrix.

VI. RESULTS AND DISCUSSION

A. Longitudinal Cooling Homogeneity

As shown in Fig. 8. Direct cooling produced significant temperature deviations along the tool. For the nominal test:

- Upper sensors (Down): 4–10 °C, RMSE = 5.11 °C
- Upper sensors (Down) with impinging jets: ≤2.4 °C, RMSE = 2.08 °C
- Lower sensors (Up): 6.8 °C with direct water vs. ≤3.8 °C with jets, RMSE = 2.7 °C

This corresponds to 59% improvement above the channel and 55% below, confirming jet impingement effectively redistributes heat transfer along the channel.

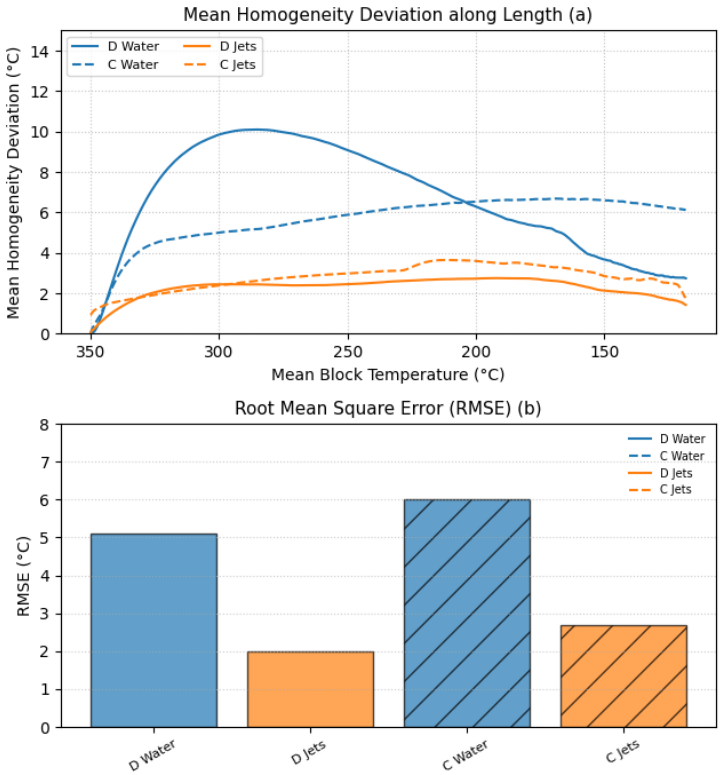

Fig. 8. Temperature deviation along the channel: (a) mean deviation; (b) RMSE for both cooling configuration.

B. Predictive Control Performance

The ARMAX-based MPC was tested on a cooling phase of thermal cycle representing composite molding (Fig. 9.):

1. Heating: Mold up to 350 °C
2. Temperature homogenization: Maintain for 15 min
3. Fast cooling: 10 °C/min to 220 °C
4. Controlled slow cooling: 1 °C/min for crystallization (PEEK 193 °C, PEI 190 °C, PET 200 °C) [20]
5. Demolding cooling: 5 °C/min to 110 °C

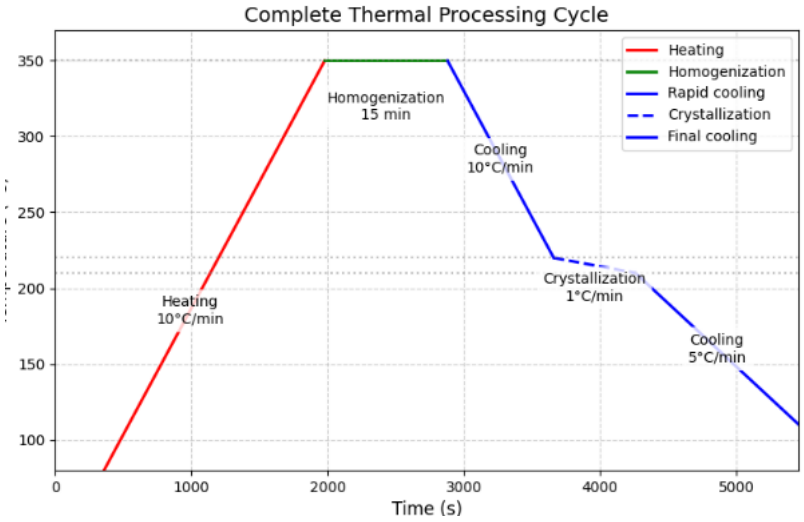

Fig. 9. Target thermal cycle for composite molding.

The subsequent Fig. 10. presents the temperature evolution for the three zones under both TOR (On–Off) and MPC control.

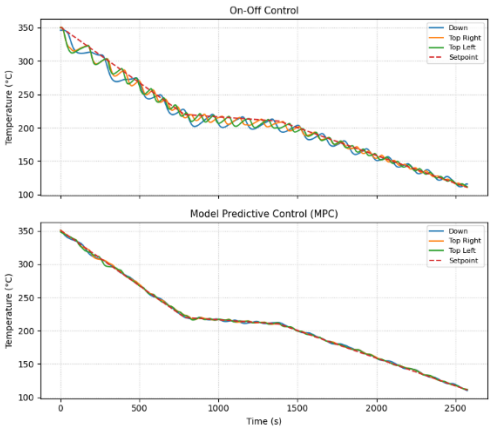

Fig. 10. Surfaces zone temperatures (A) TOR and (B) MPC.

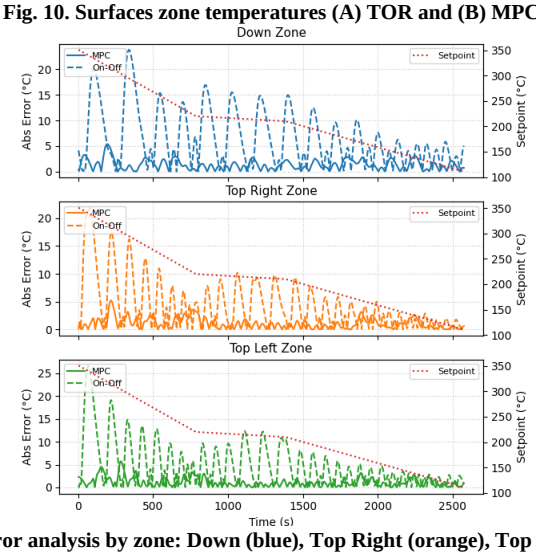

Fig. 11. Error analysis by zone: Down (blue), Top Right (orange), Top Left (green).

To better visualize tracking errors by zone, Fig. 11. presents detailed error analysis for Down (blue), Top Right (orange), and Top Left (green).

- On–Off: temperature deviations of 15–25 °C
- MPC: maximum deviations of 2–5 °C

MPC maintains temperatures closer to the setpoint, significantly reducing overshoot and oscillations. Fig. 12 summarizes the global RMSE and water consumption by zone.

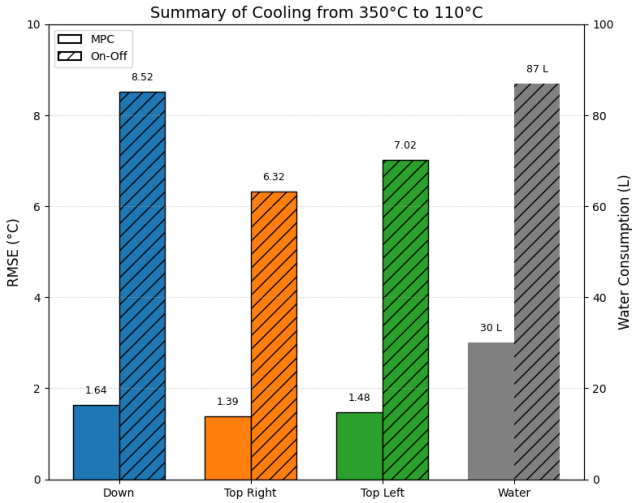

Fig. 12. Global RMSE and water consumption comparison by zone.

Improvements are:

- RMSE reduction: Down 80.8%, Top Right 78.0%, Top Left 78.9%
- Water consumption reduction: 64.8%

These results confirm ARMAX-based MPC provides accurate temperature tracking, multi-zone coordination, reduced overshoot, and efficient slow-cooling control for composite crystallization.

VII. CONCLUSION

This work presents an advanced cooling regulation strategy for composite molding tools, combining optimized impinging jet design with ARMAX-based predictive control. Key achievements:

- Enhanced thermal homogeneity along and across cooling channels
- Accurate setpoint tracking with minimal overshoot (<5 °C)
- Significant reduction in water usage (~65%)
- Adaptive performance under varying thermal and flow conditions

ARMAX-based MPC is a promising approach for next-generation intelligent molds, providing efficiency and environmental benefits. Future work will extend this methodology to large-scale tooling with multiple cooling networks and real-time adaptive learning.

REFERENCES

[1] R. F. Gibson, Principles of Composite Material Mechanics, 4th ed. Boca Raton: CRC Press, 2016. doi: 10.1201/b19626.

[2] T. K. Slange, L. L. Warnet, W. J. B. Grouve, and R. Akkerman, "Deconsolidation of C/PEEK blanks: on the role of prepreg, blank manufacturing method and conditioning," Compos. Part Appl. Sci. Manuf., vol. 113, pp. 189–199, Oct. 2018, doi: 10.1016/j.compositesa.2018.06.034.

[3] Z. J. Gombos, P. McCutchion, and L. Savage, "Thermo-mechanical behaviour of composite moulding compounds at elevated temperatures," Compos. Part B Eng., vol. 173, p. 106921, Sept. 2019, doi: 10.1016/j.compositesb.2019.106921.

[4] J. Yan, Q. Bi, Z. Liu, G. Zhu, and L. Cai, "Subcooled flow boiling heat transfer of water in a circular tube under high heat fluxes and high mass fluxes," Fusion Eng. Des., vol. 100, pp. 406–418, Nov. 2015, doi: 10.1016/j.fusengdes.2015.07.007.

[5] G. Tymen et al., "Temperature mapping in a two-phase water-steam horizontal flow," Exp. Heat Transf., vol. 31, no. 4, pp. 317–333, July 2018, doi: 10.1080/08916152.2017.1410505.

[6] J. I. Arrizubieta, M. Cortina, M. Ostolaza, J. E. Ruiz, and A. Lamikiz, "Case Study: Modeling of the cycle time reduction in a B-Pillar hot stamping operation using conformal cooling," Procedia Manuf., vol. 41, pp. 50–57, Jan. 2019, doi: 10.1016/j.promfg.2019.07.028.

[7] S. S. Deepika, B. T. Patil, and V. A. Shaikh, "Plastic injection molded door handle cooling time reduction investigation using conformal cooling channels," Mater. Today Proc., vol. 27, pp. 519–523, Jan. 2020, doi: 10.1016/j.matpr.2019.11.316.

[8] T.-W. Wei et al., "Experimental characterization and model validation of liquid jet impingement cooling using a high spatial resolution and programmable thermal test chip," Appl. Therm. Eng., vol. 152, pp. 308–318, Apr. 2019, doi: 10.1016/j.applthermaleng.2019.02.075.

[9] E. Agyeman, D. Edelin, and D. Lecointe, "Experimental Study of the Effect of a Cross Airflow on the Dynamics and Heat Transfer Performance of Impinging Circular Water Jets on a Concave Surface," Heat Transf. Eng., 2021, doi: 10.1080/01457632.2021.1887640.

[10] F. V. Barbosa, S. F. C. F. Teixeira, and J. C. F. Teixeira, "Flow dynamics and heat transfer characterization of confined multiple jets impinging on a complex surface," Exp. Fluids, vol. 64, no. 9, p. 153, Aug. 2023, doi: 10.1007/s00348-023-03692-x.

[11] D. E. Guerfi, S. Roux, N. Allanic, A. Sarda, and D. Lecointe, "Parametric Study on Enhanced Thermal Management via Regulated Impingement Boiling Cooling," J. Fluid Flow Heat Mass Transf., vol. 11, 2024, doi: 10.11159/jffhmt.2024.015.

[12] D. E. Guerfi, R. Stéphane, A. Nadine, S. Alain, and L. Damien, Optimizing Thermal Management with Regulated Jet Impingement Boiling Cooling and Transverse Airflow: A Parametric Analysis. 2024. doi: 10.11159/enfht24.273.

[13] D. E. Guerfi, "Etude d'un assemblage de modules de régulation d'outillage utilisant une technologie de refroidissement multi-jets," PhD Thesis, Nantes Université, 2025.

[14] E. K. K. Agyeman, P. Mousseau, A. Sarda, D. Edelin, and D. Lecointe, "Homogeneous and Automated Cooling of a Mold Segment by Multiple Water Jet Impingement and a Cross Air Flow," J. Therm. Sci. Eng. Appl., vol. 13, no. 061020, Apr. 2021, doi: 10.1115/1.4050569.

[15] H. Hosseinionari and R. Seethaler, "The integration of Model Predictive Control and deep Reinforcement Learning for efficient thermal control in thermoforming processes," J. Manuf. Process., vol. 115, pp. 82–93, Apr. 2024, doi: 10.1016/j.jmapro.2024.01.085.

[16] D. E. Guerfi, S. Roux, N. Allanic, A. Sarda, and D. Lecointe, "Comprehensive Analysis of Critical Heat Flux and Heat Transfers in a Confined Jet Impingement Boiling Cooling System," ASME 2024 Heat Transfer Summer Conference, Anaheim, California, USA, , Sept. 2024. doi: 10.1115/HT2024-121973.

[17] S. G. Lee, M. Kaviany, and J. Lee, "Quench subcooled-jet impingement boiling: Two interacting-jet enhancement," Int. J. Heat Mass Transf., vol. 126, pp. 1302–1314, Nov. 2018, doi: 10.1016/j.ijheatmasstransfer.2018.05.113.

[18] A. Bemporad, M. Morari, and N. Ricker, Model Predictive Control Toolbox. 2005.

[19] L. Ljung, "System Identification," in Wiley Encyclopedia of Electrical and Electronics Engineering, John Wiley & Sons, Ltd, 1999. doi: 10.1002/047134608X.W1046.

[20] Shah, V. (2006). Handbook of Plastics Testing and Failure Analysis. Wiley. doi:10.1002/0470100427

★★★